forests

MDPI

Article

Modeling Ecosystem Services for Park Trees: Sensitivity of i-Tree Eco Simulations to Light Exposure and Tree Species Classification

Rocco Pace [1], Peter Biber [2], Hans Pretzsch [2] and Rüdiger Grote [1,*]

[1] Karlsruhe Institute of Technology (KIT), Institute of Meteorology and Climate Research, Atmospheric Environmental Research (IMK-IFU), Kreuzeckbahnstraße 19, 82467 Garmisch-Partenkirchen, Germany; rocco.pace@kit.edu

[2] Chair for Forest Growth and Yield Science, Faculty of Forest Science and Resource Management, Technical University of Munich, Hans-Carl-von-Carlowitz-Platz 2, 85354 Freising, Germany; peter.biber@lrz.tu-muenchen.de (P.B.); hans.pretzsch@lrz.tu-muenchen.de (H.P.)

* Correspondence: ruediger.grote@kit.edu

Received: 18 January 2018; Accepted: 10 February 2018; Published: 13 February 2018

Abstract: Ecosystem modeling can help decision making regarding planting of urban trees for climate change mitigation and air pollution reduction. Algorithms and models that link the properties of plant functional types, species groups, or single species to their impact on specific ecosystem services have been developed. However, these models require a considerable effort for initialization that is inherently related to uncertainties originating from the high diversity of plant species in urban areas. We therefore suggest a new automated method to be used with the i-Tree Eco model to derive light competition for individual trees and investigate the importance of this property. Since competition depends also on the species, which is difficult to determine from increasingly used remote sensing methodologies, we also investigate the impact of uncertain tree species classification on the ecosystem services by comparing a species-specific inventory determined by field observation with a genus-specific categorization and a model initialization for the dominant deciduous and evergreen species only. Our results show how the simulation of competition affects the determination of carbon sequestration, leaf area, and related ecosystem services and that the proposed method provides a tool for improving estimations. Misclassifications of tree species can lead to large deviations in estimates of ecosystem impacts, particularly concerning biogenic volatile compound emissions. In our test case, monoterpene emissions almost doubled and isoprene emissions decreased to less than 10% when species were estimated to belong only to either two groups instead of being determined by species or genus. It is discussed that this uncertainty of emission estimates propagates further uncertainty in the estimation of potential ozone formation. Overall, we show the importance of using an individual light competition approach and explicitly parameterizing all ecosystem functions at the species-specific level.

Keywords: air pollution removal; BVOC emission; carbon sequestration; tree competition; urban forest

1. Introduction

Population growth, climate change, and high and increasing air pollution levels are known to pose risks to health and safety in cities [1]. Therefore, sustainable urban planning is necessary to improve the quality of life and preserve the integrity of natural ecosystems [2]. Urban forests and trees can significantly contribute to mitigating climate change effects and improving air quality in residential areas [3]. Pollution caused by tree removal in cities considerably depends on the species

and their properties [4]. For this reason, species selection is important to achieve optimal results of city greening [5]. To find the most suitable trees or tree mixture, ecosystem services models can be particularly useful as decision-support tools for city planning [6,7].

The i-Tree Eco model is an ecosystem service model for urban trees developed by the US Department of Agriculture (USDA) Forest Service for application in the U.S., and it has been adopted by the U.K., Australia, and Canada [8,9]. The model is widely used to evaluate urban vegetation-induced environmental services [10–12], e.g., carbon storage and sequestration, air pollution reduction, and water runoff reduction, the effects of trees on energy consumed by buildings, and some disservices, such as the emission of biogenic volatile organic compounds (BVOCs).

The i-Tree Eco requires information concerning the species and the stem diameter at breast height (DBH) as the input data. Additional data, including land use criteria, total tree height, crown size (height to live top, height to the crown base, crown width, and percentage of crown missing), crown health (dieback or condition), and competition status, can improve the model accuracy. Most of these input data are usually determined in the field by explicit visual inventories. This determination method is relatively easy to learn but remains subjective and prone to errors. For large areas, sample plots are required to be investigated and scaled to the whole region, leading to considerable uncertainties when the species distribution is non-homogeneous [13]. In addition, the efforts involved in defining the sample plots, educating the field researchers, and applying the inventory requires more time and money [14] compared to the case wherein the i-Tree Eco protocol, which refers to the data available from remote sensing or GIS, is used. The latter facilitates the assessment of pollution reduction in cities using the input of leaf area index (LAI) as a structural characteristic [15–18]. However, it is worth noting that in many cases, urban forest inventories are unsuitable for deriving all the required parameters, e.g., crown light exposure (CLE), making the use of default model parameterization for many tree properties more appealing.

Species characterization data is important for i-Tree Eco initialization because these data define the basic parameters used for calculating all ecosystem services and disservices (e.g., leaf area (LA), leaf biomass, allometric equations, BVOCs emission rates). If the species information is not available, the i-Tree Eco model uses values that are defined by the genus, family, or type (evergreen/deciduous). This may be particularly problematic if the model is applied to regions other than the U.S., for which the parameters were designed. Another important characterization is the degree of competition that a tree experiences. This is expressed as "CLE" in the i-Tree Eco model based on a visual estimate according to Bechtold (2003) [19]. Because this parameter is evaluated by educated investigators, it is expensive and remains subjective. The default value for the competition is differentiated into street trees and trees within urban parks and forests but is independent of size or closeness to neighbors. Hence, it is desirable to define i-Tree Eco initialization for species, size, and composition of each tree using cost-effective and objective methods, particularly when large areas are concerned.

A promising approach to achieve an automated initialization is the application of remote sensing methods, which has been attempted in recent investigations [15,20–22]. However, because of the complexity associated with urban areas (e.g., high spectral similarity of vegetation types or overlooked small trees in high-density stands), initializations using remote sensing data have an inevitable degree of uncertainty concerning species differentiation [23]. Additionally, it should be considered that most urban trees are deciduous [4,24]. This creates difficulties in species distinction because the photogrammetric interpretation of aerial photographs generally allows only the separation of evergreen from deciduous trees, particularly when the plant species diversity is as high as that in the urban context [25]. Furthermore, although tree position and size can be reasonably well determined, automatic information on light competition between trees is not provided by these approaches [26,27].

The actual competition between trees has been estimated using multiple approaches. These estimations include the influence zone of each tree and the degree and nature of interaction [28]; a competition algorithm based on light intensity [29]; the "moving average autoregression" method to assess the spatial dependence attributable to the competition and micro-site influences [30]; and the

calculation of the inter-tree competition between each tree based on the position, height, and crown size of a tree and its competitors [31]. The aforementioned methods provide objective measures because they are based on tree position and size, i.e., the remote sensing data.

Herein, we propose a methodology to derive competition data from dimensional tree information and investigate uncertainties inherent in i-Tree Eco model applications related to species determination. Therefore, we apply the model to Englischer Garten—a large urban park in Munich, Germany—where detailed inventory data are available, to assess how the estimates of ecosystem services and disservices change when we gradually decrease the degree of initialization detail. In particular, we hypothesized that accurate species information is crucial for determining several ecosystem processes and functions.

2. Materials and Methods

2.1. Site Description and Model Inputs

In this study, we analyzed the south of "Englischer Garten", a 330-ha park located in Munich, Germany (Figure 1). The site is mainly comprised of a mix of deciduous trees dominated (≈77%) by the species Norway maple (*Acer platanoides* L.), European beech (*Fagus sylvatica* L.), small-leaved lime (*Tilia cordata* MILL.), sycamore maple (*Acer pseudoplatanus* L.), and European ash (*Fraxinus excelsior* L.). Evergreen species contribute less than 1% to the total tree number (Table 1). The inventory comprises 9391 trees growing within the "Englischer Garten" park, which have been collected by the Bavarian Administration of State-Owned Palaces, Gardens and Lakes. These tree data (species, tree height, DBH, crown diameter, and height to the crown base) were used as input parameters in i-Tree Eco to calculate the ecosystem services provided by the park. Since information about the crown condition has not been collected, we assumed a crown condition involving the best tress, i.e., 0% crown missing and 100% healthy (or 0% dieback). Further, these input parameters can be used for increasing the accuracy of LA and carbon sequestration estimations [32].

Table 1. Species composition of the south part of Englischer Garten (a total of 9391 trees).

Species	Relative Number (%)	Basal Area (m^2)
Norway maple (*Acer platanoides* L.)	32.9	453.6
European beech (*Fagus sylvatica* L.)	12.6	447.4
Small-leaved lime (*Tilia cordata* MILL.)	11.2	160.1
Sycamore maple (*Acer pseudoplatanus* L.)	10.4	122.8
European ash (*Fraxinus excelsior* L.)	10.1	223.2
Field maple (*Acer campestre* L.)	3.7	35.8
European hornbeam (*Carpinus betulus* L.)	3.6	43.6
Horse-chestnut (*Aesculus hippocastanum* L.)	2.6	70.1
English oak (*Quercus robur* L.)	2	32.4
Scotch elm (*Ulmus glabra Huds.*)	1.8	28.8
Black locust (*Robinia pseudoacacia* L.)	1.6	21.7
London plane (*Platanus* × *acerifolia Aiton*)	1.3	19.4
White willow (*Salix alba* L.)	1.0	43.3
Willows (*Salix* spp.), poplars (*Populus* spp.), cherries (*Prunus* spp.), Caucasian wingnut (*Pterocarya fraxinifolia*), birches (*Betula* spp.), hazels (*Corylus* spp.), walnuts (*Juglans* spp.), common pear (*Pyrus communis*), honey locust *Gleditsia triacanthos*, tulip tree (*Liriodendron tulipifera*), hawthorns (*Crataegus* spp.), ginkgo (*Ginkgo biloba*), whitebeams (*Sorbus* spp.), grey alder (*Alnus incana*), tree of heaven (*Ailanthus altissima*), cornelian cherry (*Cornus mas*), Japanese pagoda tree (*Sophora japonica*), yew (*Taxus baccata*), pines (*Pinus* spp.), and spruce (*Picea abies*), magnolia (*Magnolia* spp.)	5.2 (evergreen species <1%)	82.6

The model simulations were conducted in 2012 using hourly meteorological data registered at the Munich Airport (temperature, wind speed, and radiation from the National Oceanic and Atmospheric Administration (NOAA, Silver Spring, MD, USA) database that is directly accessed by i-Tree Eco, Farnham, UK) and the München Theresienstrasse (precipitation) weather stations, which are about 40 and 1 km away from the study site, respectively. The average hourly concentration data for ozone (O_3), sulfur dioxide (SO_2), nitrogen dioxide (NO_2), carbon monoxide (CO), and particulate matter with

a diameter of 2.5 ($PM_{2.5}$) were provided from the Bavarian Environment Agency (LFU), Augsburg, Germany. PM_{10} data are no longer analyzed in the latest i-Tree Eco version (version 6) because $PM_{2.5}$ is generally more relevant for human health [33]. This information was checked for quality and fed into the USDA Forest Service database for its use in our investigation.

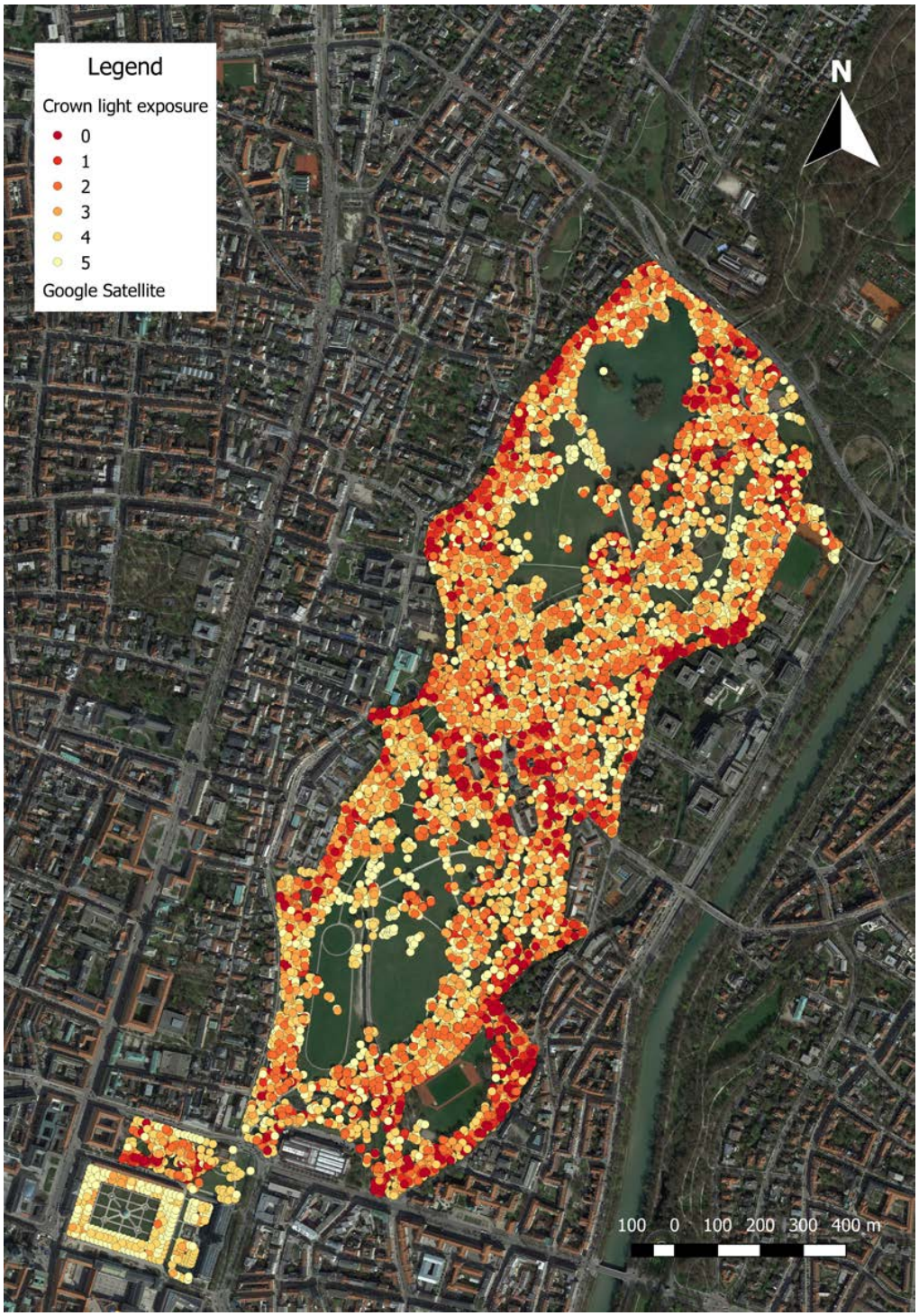

Figure 1. All trees in the south of Englischer Garten with relative crown light exposure (CLE) classes calculated by the CCS (crown competition for sunlight) competition index which is based on the algorithms provided in Pretzsch et al. [31]. In addition to competition between trees, shading by buildings has been considered as well.

2.2. CLE Effects

The i-Tree Eco model considers the average competition of a tree as the degree of crown exposure to sunlight, which is not supposed to change during the simulation. This competition is expressed as CLE (crown light exposure), which is an empirical index that reflects the number of sides of a tree receiving direct sunlight [32]. Therefore, the tree crown is virtually divided into the four cardinal directions and an additional surface on top of the crown (Figure 2) [19]. A classification can thus result in a CLE value between 0 (which would characterize a fully suppressed tree in the understorey of a closed canopy, only receiving diffuse light) and 5 (solitary tree not shaded by surrounding trees or other obstacles). CLE reflects broadly the capability for photosynthesis and is used to calculate LA and tree growth estimates. While growth directly determines carbon sequestration, LA influences various ecosystem services. Herein, we investigate air pollution reduction and biogenic emissions to determine the CLE sensitivity (see Section 2.4).

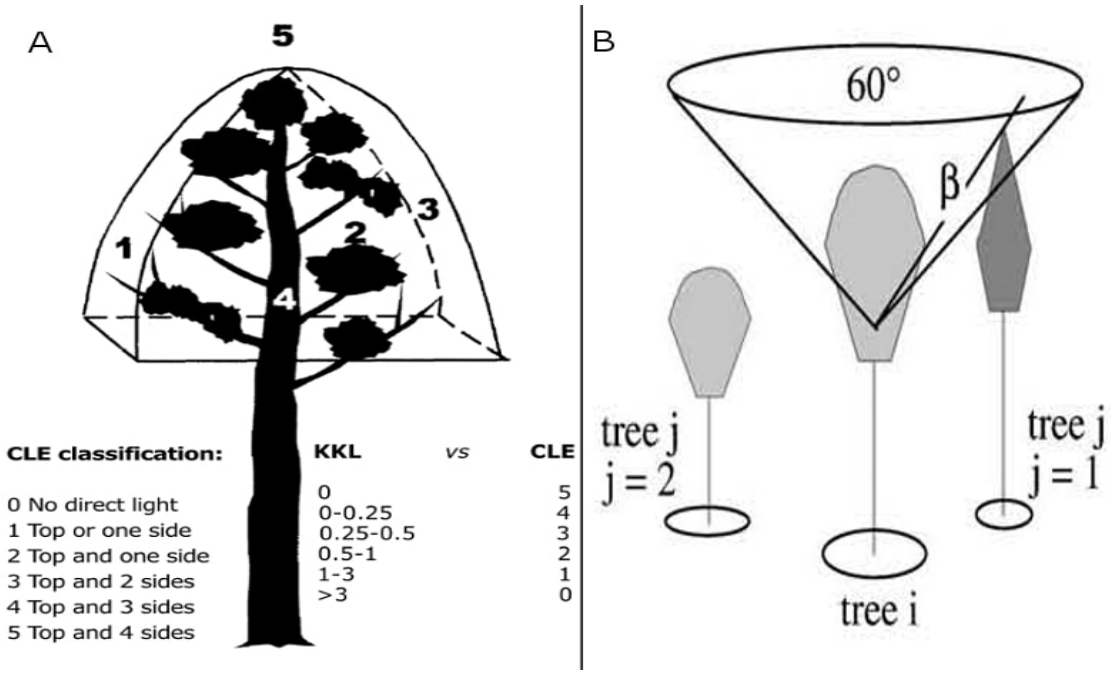

Figure 2. Crown light exposure (CLE) classification (**A**) and calculation of the competition index CCS (crown competition for sunlight) based on Pretzsch et al. (**B**). In the bottom right corner of (**A**), the conversion of CCS is indicated in CLE values. Sources: [19,31].

2.2.1. Calculation of Leaf Area (LA)

The i-Tree Eco model uses tree-specific CLE values that are grouped into three states in order to calculate LA: the open-grown (CLE = 4–5), park (CLE = 2–3), and closed forest (CLE = 0–1) conditions. Under the open-grown condition, LA is calculated either from DBH only (measured at 1.37 m above ground) or from crown length (H) and crown width (D) if available [34]:

- CLE = 4–5 (open-grown trees)

$$\ln(\mathrm{LA}) = b_0 + b_1\mathrm{DBH} + b_2\mathrm{S} \quad (1)$$

$$\ln(\mathrm{LA}) = b_0 + b_1\mathrm{H} + b_2\mathrm{D} + b_3\mathrm{S} + b_4\mathrm{C} \quad (2)$$

In these calculations, S is a species-specific shading factor, which is defined as the percentage of light intensity intercepted by foliated tree crowns, and C is the outer surface area of the tree crown calculated from H and D as $C = \pi D(H + D)/2$. S varies with species for deciduous trees, and if it is not

defined for individual species, the averages for the genus or general hardwoods are used. For conifer trees, the model applies a shading factor of 0.91 for all species, except for pines (0.83) [32,34]. For the closed forest condition, LA is calculated using the following equation based on the Beer-Lambert law:

- CLE = 0–1 (forest stand condition)

$$LA = (\ln(1 - S)/-k) \times \pi \times (D/2)^2 \quad (3)$$

where k is a light extinction coefficient that is differentiated between conifers (0.52) and hardwoods (0.65) [32]. For CLE = 2–3 (park condition), LA is calculated as the average value determined by the open-grown (CLE = 4–5) and closed canopy equations (CLE = 0–1).

2.2.2. Effects on Tree Growth

Average diameter growth is added to tree diameter (year x) to estimate the tree diameter in year x + 1 [35]. In i-Tree Eco, a standard diameter growth (SG) that can be reduced is defined for open-grown trees (CLE = 4–5) when the number of frost-free days is smaller than a defined value:

$$\text{Standard diameter growth (SG)} = 0.83 \text{ cm/year} \times (\text{number of frost-free days}/153) \quad (4)$$

Park tree growth (CLE = 2–3) is calculated by dividing SG of open-grown trees by 1.78 and that of forest trees (CLE = 0–1) by 2.29.

2.2.3. Automated Competition Calculations

Herein, we calculated CLE based on a routine introduced within the framework of the single-tree-based stand simulator SILVA [31]. This model calculates single-tree growth in relation to its surrounding three-dimensional space to produce the competition index *CCS* value. *CCS* aids in identifying the competitors of single trees by considering a virtual reverse cone with an axis equal to the tree axis and its vertex placed within the crown of the tree (Figure 2b). The model determines the angle β between the insertion point of the cone and the top of any competitor tree. This angle is multiplied by the crown cross-sectional areas (CCAs) of the competitors and the tree of interest considering a species-specific light transmission coefficient:

$$CCS_i = \sum_{j=1}^{n} \left(\beta_i \frac{CCA_j}{CCA_i} TM_j \right) \quad (5)$$

where CCS_i is the competition index for tree i; β_i is the angle between cone vertex and top of competitor j; CCA_j and CCA_i are the *CCAs* of trees j and i, respectively; TM_j is the species-specific light transmission coefficient for tree j; n is the number of competitors of tree i [31].

We calculated the competition index *CCS* for each tree before converting the results into a CLE classification. Therefore, we assumed that the trees without competition (*CCS* = 0) correspond to the highest CLE value (CLE = 5), while other CLE classes are assigned to *CCS* values according to the relative abundance of trees (see Figure 2a). Thus, there is approximately the same number of trees in each CLE class. We also considered shading by buildings and other trees not included in our inventory using the open source Quantum GIS (QGIS) software and a fixed buffer distance of 15 m around the trees. For all trees falling within this distance, we reduced the CLE by one unit.

2.3. Model Sensitivity Studies

The importance of individually determined CLEs was tested by comparing simulated carbon sequestration, pollution reduction, and emissions calculated using the SILVA routine (indicated as individual CLE runs) with the results originating from default CLE values (indicated as average CLE runs). The sensitivity connected to uncertain tree species determination was also investigated by deriving parameters from different information sources: (1) individually determined tree species

through field measurements (species-specific runs); (2) assuming a genus-specific inventory that reflects the detail derived by, for example, sophisticated remote sensing techniques, such as LiDAR (light detection and ranging) and high-resolution images (genus-specific runs) [23]; and (3) assuming a distinction between evergreen and deciduous trees representing the detail that can be derived by photogrammetric interpretation of aerial photographs (dominant species runs) [25]. In this context, we hypothesized that all deciduous species were *A. platanoides*, the dominant species of the park (Table 1), and all evergreen trees had the properties of *Picea abies*, the most common conifer species in South Germany [36].

2.4. Model Calculations

For all calculations, the initial dimensional data, hourly temperature and precipitation records, and air pollution concentrations are used as input data [32,37]. Only ecosystem services with a direct link to air chemistry, i.e., air pollution reduction, carbon sequestration, and biogenic emissions, were evaluated. In subsequent paragraphs, we describe how the model calculates these services.

2.4.1. Carbon Storage and Sequestration

The model calculates the above-ground biomass of trees in dry weight using allometric equations [35,38] and the total tree biomass using a root-to-shoot ratio of 0.26 [32,39]. Because the allometric equations are diameter-based and developed for closed canopies, biomass should be corrected for open-grown trees, which tend to be shorter and thus have less above-ground biomass at a given diameter. Therefore, biomass estimates are reduced for urban trees by a factor of 0.8 [38]. Total carbon storage is calculated by multiplying tree dry weight biomass by 0.5 [32]. Hence, assuming that there is no change in soil carbon, annual carbon sequestration is directly calculated from tree growth (see Section 2.2.2) [32].

2.4.2. Air Pollution Reduction

The dry deposition of O_3, SO_2, NO_2, CO, and $PM_{2.5}$ is hourly determined throughout the year [40–43]. During precipitation events, deposition is assumed to be zero. Using the following equation, for other periods, the pollutant flux into the biosphere (F; in g m^{-2} s^{-1}) is calculated as the product of deposition velocity (V_d; in m s^{-1}) and pollutant concentration (C; in g m^{-3}) [41]:

$$F = V_d\, C \tag{6}$$

Using the following equation, the deposition velocities of CO, NO_2, SO_2, and O_3 are calculated as the inverse of the sum of the aerodynamic resistance R_a, a quasi-laminar boundary layer (R_b), and the canopy resistance R_c expressed in s m^{-1} [44]:

$$V_d = (R_a + R_b + R_c)^{-1} \tag{7}$$

where R_a is determined from meteorological data (wind speed and atmospheric stability) since it is assumed to be independent of air pollution type or plant species, R_b is based on a value defined in a study by Pederson et al. (1995) [45] using a specific Schmidt number for each air pollutant [46], and R_c is calculated using the following equation:

$$1/-R_c = 1/(r_s + r_m) + 1/r_{soil} + 1/r_t \tag{8}$$

where r_s is the stomatal resistance (s m^{-1}), r_m is the mesophyll resistance (s m^{-1}), r_{soil} is the soil resistance (2941 s m^{-1} in growing season and 2000 otherwise), and r_t is the cuticular resistance (s m^{-1}).

Hourly canopy resistance values for O_3, SO_2, and NO_2 were calculated based on a modified hybrid of big leaf and multilayer canopy deposition models [44,47]. The model calculates stomatal resistance (r_s) as the inverse of stomatal conductance, which is estimated based on the leaf photosynthetic rate,

relative humidity, and surface CO_2 concentration using the Ball-Berry formula (for more details, see [46]). The mesophyll and cuticular resistance values are set based on those reported in the literature: for NO_2, r_m = 100 s m^{-1} [48] and r_t = 20,000 s m^{-1} [49]; for O_3, r_m = 10 s m^{-1} [48] and r_t = 10,000 s m^{-1} [50,51]; and for SO_2, r_m = 0 [49] and r_t = 8000 s m^{-1}. As CO reduction is assumed to be independent of photosynthesis and transpiration, the resistance value for CO is set to 50,000 s m^{-1} in the in-leaf season and 1,000,000 s m^{-1} in the out-leaf season for all trees [52]. The hourly deposition and resuspension rates for $PM_{2.5}$ are calculated based on wind speed and LA (for more details, see [42]).

The base deposition velocity V_d was multiplied by the individual tree LAI based on local field data and local seasonal variation (local leaf-on and leaf-off dates). For deciduous trees, the calculation of pollution deposition is limited to the in-leaf period. Herein, the leaf-on date is 5 April, whereas the leaf-off date is October 28.

2.4.3. Biogenic Emissions

Hourly emissions of isoprene (C_5H_8) and monoterpenes (C_{10} terpenoids) were estimated using an approach proposed by Guenther et al. 1993 [53] and Geron et al. 1994 [54] with genus-specific parameters [55]. In this approach, emission was calculated by multiplying leaf biomass (derived from LA with species-specific conversion factors) by emission rates. These in turn depend on temperature and light (isoprene) or temperature only (monoterpenes) as well as on genus-specific factors that represent emissions at 30 °C and 1000 µmol m^{-2} s^{-1} photosynthetically active radiation (PAR) [56]. Median emissions values for the family, order, or superorder were used if genus-specific emission was not available [32]. Incoming PAR was calculated as 46% of total solar radiation input [57]. Because isoprene emission has a nonlinear dependence on light, PAR was estimated from incoming PAR for 30 canopy levels using the sunfleck canopy environment model with the LAI of the analyzed structure [32]. Hourly leaf temperature was calculated from air temperature while considering the transpiration rate (for unlimited water supply), LAI, and percentage tree cover [55].

3. Results

3.1. Ecosystem Services

The tree crowns of Englischer Garten were calculated to cover an area of 73.2 ha and have a total LA of 467.5 ha with a leaf biomass of 301.7 tons. The most dominant species in terms of number and basal area were *A. platanoides* and *F. sylvatica* (Table 1). Overall, carbon stored in the trees was estimated to be 6225 tons. In accordance with their fraction of basal area, *F. sylvatica* and *A. platanoides* stored the most carbon (31.4% and 29.1% of the total, respectively). The amount of carbon sequestered in 2012 was calculated to be 214 tons (Figure 3). The model further indicates that the trees in Englischer Garten removed 2610 kg of O_3, 845 kg of NO_2, 186 kg of $PM_{2.5}$, 171 kg of SO_2, and 62 kg of CO (Figure 4). In addition, the trees emitted an estimated BVOC amount of 550 kg (158 kg isoprene and 392 kg monoterpenes; Figure 5).

3.2. Sensitivity to Average CLE Values

Simulation with average CLE values (CLE average) resulted in a 14% reduction in LA and leaf biomass (379.9 vs. 443 ha $year^{-1}$; 224.9 vs. 262 t $year^{-1}$) compared to the run with individual determination of CLE (Figure 3). This directly affected bioemissions (494 vs. 550 kg $year^{-1}$; Figure 5) and pollution reduction (Figure 4). Except for CO (in both cases, 62 kg $year^{-1}$), more pollutants were removed in the "CLE individual" simulation compared to the "CLE average" simulation (2610 vs. 2482 kg $year^{-1}$ for O_3, 845 vs. 794 kg $year^{-1}$ for NO_2, 186 vs. 165 kg $year^{-1}$ for $PM_{2.5}$, and 171 vs. 164 kg $year^{-1}$ for SO_2). Carbon sequestration was also affected by individual light exposure (Figure 3): 214 tons of carbon (784 CO_2 equivalent) removed in the "CLE individual" simulation compared to 155 tons of carbon (567 CO_2 equivalent) removed in the "CLE average" simulation, indicating that the trees in Englischer Garten were more open grown than expressed by the average CLE value.

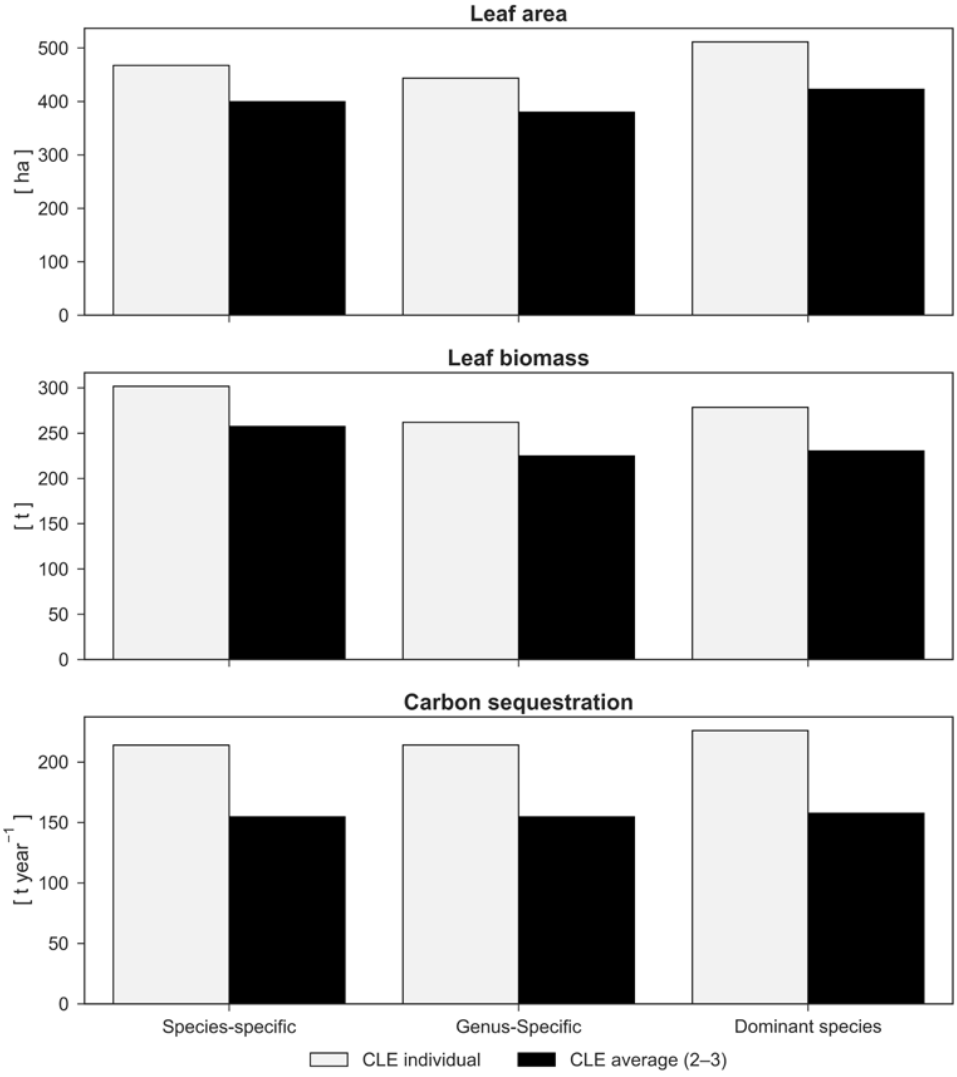

Figure 3. Leaf area (LA), leaf biomass, and carbon sequestration comparison between the "species-specific", "genus-specific", and "dominant species" simulations considering the crown light exposure (CLE) value for each tree (CLE individual) and the average CLE values (CLE average).

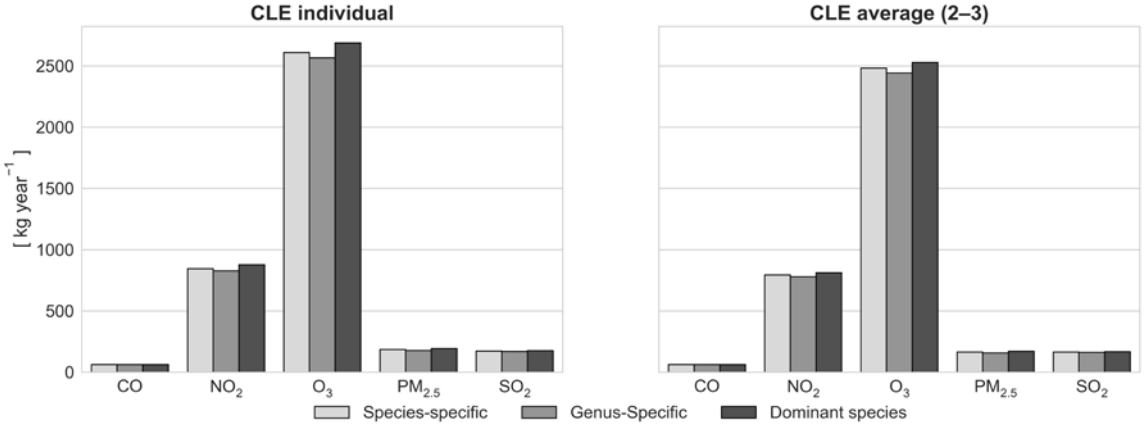

Figure 4. Air pollution reduction comparison between the "species-specific", "genus-specific", and "dominant species" simulations considering the crown light exposure (CLE) for each tree (CLE individual) and the average CLE values (CLE average).

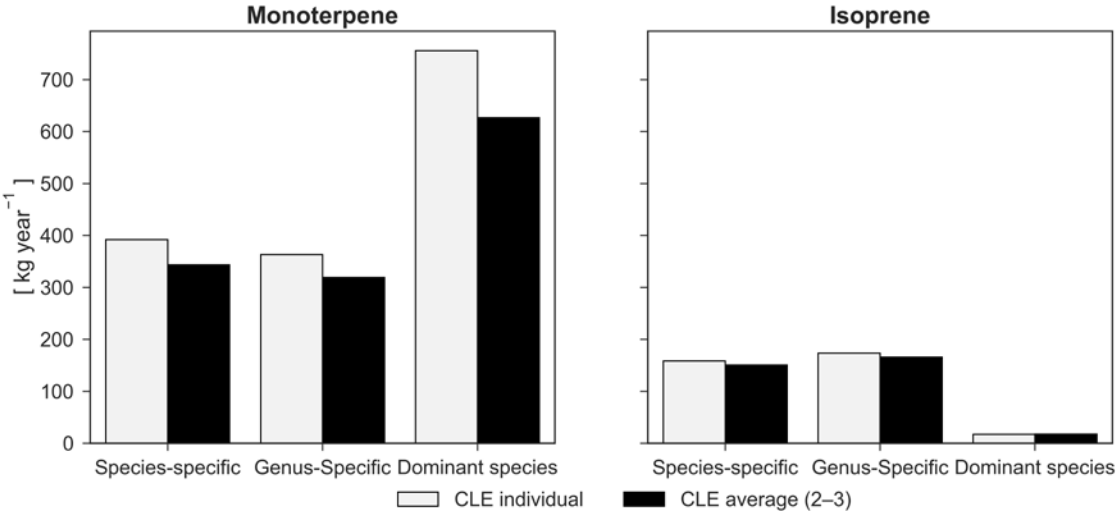

Figure 5. Comparison of monoterpene and isoprene emissions between the "species-specific", "genus-specific", and "dominant species" simulations considering the crown light exposure (CLE) for each tree (CLE individual) and the average CLE values (CLE average).

3.3. Sensitivity to Different Species Classification

Compared to simulations with species-specific parameterization, the results obtained with the genus-specific simulation showed lower LA (−5%; 443.7 ha) and leaf biomass (−13%; 262 t). The dominant species simulation demonstrated higher LA values (511.3 ha; 9% higher than the species-specific parameterization), but leaf biomass results (−8%; 278.4 t) were almost equivalent (Figure 3).

According to lower LA, pollutants removed with genus-specific parameterization were fewer than those removed with species-specific parameterization (−2% of O_3, −2% of NO_2, −5% of $PM_{2.5}$, and −1% of SO_2), except for CO (62 kg year^{-1}), as shown in Figure 4. The effects of species differentiation were small. LA also had a minor effect on BVOC emissions, which are otherwise driven by marginally different parameters for the species- and genus-specific simulations. However, when the parameters were set according to the dominant species approach, monoterpene emissions were considerably higher (+93%) and isoprene emissions tended to be zero (−89%) compared to the species-specific simulation.

Carbon sequestration (214 t) was not altered by the species- and genus-specific parameterizations because biomass growth was found to solely depend on the tree size and competition state (Figure 3). Instead, the dominant species simulation showed higher carbon sequestration (+5.7%; 226 t). In this case, a larger number of trees fell into class 4–5 due to the smaller transmission coefficients for maples in comparison with the species average (Figure 6).

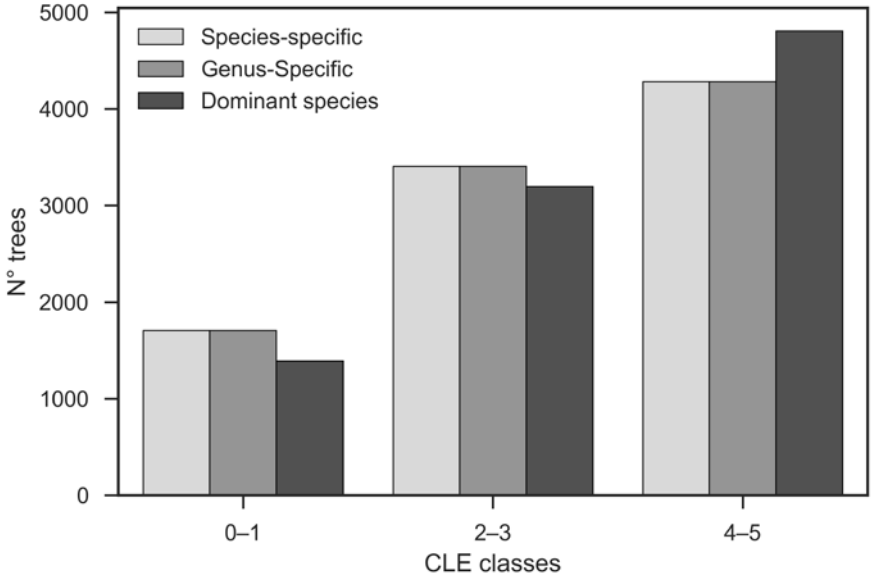

Figure 6. Comparison of crown light exposure (CLE) classes between the "species-specific", "genus-specific", and "dominant species" simulations. Class 4–5 (open-grown trees) is dominant in all simulations, particularly in the "dominant-species" simulation (99.4% of *Acer platanoides*).

4. Discussion

Our investigation demonstrates that Englischer Garten—a major park in Munich—provides a considerable amount of environmental services, i.e., air pollution reduction and carbon sequestration. Simulated removals of O_3 and NO_2 were at the highest rates (3.6 and 1.1 g m^{-2}, respectively). A comparison with the estimates for other European cities showed that the total pollutant (combining CO, O_3, NO_2, SO_2, and $PM_{2.5}$) removal rate, which was 5.3 g m^{-2} of tree cover per year, was similar to that for the city of Strasbourg (5.1 g m^{-2}) [12] but lower than that for London (8.7 g m^{-2}) [58]. The simulated $PM_{2.5}$ removal rate for the park (0.25 g m^{-2}) was of the same magnitude as that determined for U.S. cities (0.25 g m^{-2}) [42], but the total removal rate (considering $PM_{2.5}$ instead of PM_{10}) was lower than the average value calculated for the U.S. cities (7.5 g m^{-2}) [41].

Although we focused on uncertainties associated with parameterization and the determination of light competition (discussed further below), we also addressed the process uncertainty that is tightly linked to parameterization because processes and parameters often share the same knowledge base. Other uncertainties associated with the model inputs were climate conditions, which resulted in different degrees of ecosystem services during different years, and air pollution data measured outside the park, which may not reflect the ambient conditions of the park trees. However, since these aspects do not alter the relative contribution to the ecosystem services of different tree species, their investigation was outside the scope of this study.

4.1. Uncertainties Associated with Parameterization

Species definition is fundamental information on which many properties depend. Therefore, we introduced a degree of uncertainty in species definition based on either imperfect knowledge—as is often the case with species in areas outside the original model development region (genus-specific parameterization)—or what can reasonably be derived from remote sensing measures (dominant species parameterization).

The total LA in the "genus-specific" simulation was approximately 5% lower than that in the "species-specific" simulation, which slightly reduced pollution removal. This reflects the similarity between species- and genus-based parameters, exhibiting the almost linear scaling of LA and deposition in i-Tree Eco. The differences are more comprehensively expressed with BVOC emissions

that are higher for isoprene (+10%) and lower for monoterpene (−7%) using only genus-specific parameterization. This highlights the additional influence of species-specific conversion factors between LA and leaf biomass. However, there were no differences between the two simulations concerning carbon sequestration because it is based on a fixed diameter growth rate and allometric equations from the literature that are used to calculate biomass change from the dimensional change [38,56]. Such allometric equations are usually derived from forest trees and, although they have been adjusted for urban conditions, they might not exactly reflect the actual tree forms and wood density. For example, various investigations show that high ozone concentration can cause a reduction in the root/shoot ratios of trees [59], especially for deciduous species [60]. Under high air pollution a larger root biomass fraction can thus be expected.

This approach might be improved by introducing a dependency on climate and soil type, particularly by encompassing drought stress events [61] and other stress factors that might depend on the degree of air pollution or salt application. Pretzsch et al. (2017) [62] showed that the urban trees in Europe have accelerated their growth since 1960 because of the effects of climate change, with considerable differences in different climate regions. Dahlhausen et al. (2017) [63] demonstrated the effect of urban climate on lime tree growth in Berlin and found that the trees in the city center were more responsive than those in urban boundaries. It is a challenge to represent these findings with the i-Tree Eco model by only considering the limited number of frost-free days, as is currently the case. Instead, representing the growth demands the introduction of direct sensitivity to temperature, competition, and possibly other factors that will vary from those of the city of interest. In addition, wood density and growth form might require parameterization that is regionally adapted to European species [64,65].

The dominant species parameterization assumes all deciduous trees (99.4% of total population) to be Norway maple (*A. platanoides*) and uses the parameters of spruce (*P. abies*) for all the evergreen trees (0.6%). Although the effects were found to strongly depend on the species composition and the dominant species used for representation, the results showed that tree species misclassification particularly affects BVOC emission estimates. Additionally, important information concerning LA and related air pollution reduction rates was derived. The effect of parameterization on emissions was expressed because emissions factors change strongly between species. For example, high monoterpene emissions resulted from *A. platanoides*—a dominant species having one of the highest monoterpene emission factors (1.6) of all species in the inventory (0.6 for *Fagus*, 0.1 for *Fraxinus*, and 0 for *Tilia*). In contrast, maples had a considerably low isoprene emission factor (0.1) compared to that of a number of species that were neglected in the dominant species runs, reducing the overall emission estimate for this compound. For example, *Quercus robur*, *Robinia pseudoacacia*, *Platanus* × *Acerifolia*, and *Salix alba* were all assumed to be considerably high isoprene emitters (with emission factor equal to 70) [56].

However, it is worth noting that emission parameters are uncertain. For example, monoterpene emission factors reported in the literature vary between 0.1 [66] and 43.5 [67] for *Fagus*, between 0 [68] and 9.6 [69] for *Fraxinus*, and between 0 [70] and 1.2 [71] for *Tilia*. For subtropical street trees, Dunn-Johnston et al. (2016) [72] showed that a considerable difference exists between species-derived isoprene emission rates and those assumed (genus-specific emission rates) in i-Tree Eco. Other uncertainties in the emission pattern of plants were found to originate from seasonal changes that depended on the weather conditions of the previous days and weeks [73], which were not considered herein. Additionally, the potential effects of air pollution [74] or drought [75,76], which might increase or decrease emissions, have been neglected. Since emissions are supposed to trigger aerosol production and ozone formation [77], these deficits may need consideration in order to be appropriately used in combination with regional air chemistry and climate models [78].

4.2. Uncertainties Associated with Competition Calculations

Another form of influential information is the determination of competition, which represents the light that an individual tree is able to utilize during photosynthesis. We demonstrated that neglecting

an individual CLE determination (CLE average) strongly affected LA and thus pollution reduction (except for CO), carbon sequestration, and bioemissions. The intensity of this effect depended on the degree to which tree size and position differed from a homogeneous distribution with medium tree distances. Free-standing trees requiring more sunlight are therefore underrepresented in terms of LA and growth when only using average CLE determination [79]. Since Englischer Garten is characterized by many open spaces and areas where trees are found to clump together, the divergence from the mean conditions is relatively large (Figure 6). However, this is not an exception, since parks are often characterized by a complex tree distribution pattern in order to optimize recreational activities [3]. Therefore, we assumed that the structure of the Englischer Garten park was representative and that the significance of considering individual crown exposure was possibly high.

It is worth noting that the uncertainties associated with competition estimates can multiply with those associated with parameter estimation. In our case, the difference between the individual and mean competition calculations was particularly high when only "dominant species" parameters were used: the class with average competition (CLE = 2–3) was 56% larger than that with high competition (CLE = 0–1) and 51% smaller than that with low competition (CLE = 4–5) (50% and 26% for the species- and genus-specific simulations, respectively; Figure 6). Part of this effect was due to the method we designated CLE classes from competition calculations. Because competition depends on transmission properties of the canopy that differ with species, dominant-species parameterization results in different tree numbers per CLE class than species- or genus-specific parameterization (no difference exists between those two since light transmission factors are homogeneous within a genus) [31].

4.3. Uncertainties Associated with Processes

Pollution deposition was calculated from LA and species-specific deposition velocities. However, uptake processes may need to be differentiated in terms of stomatal uptake and deposition onto the surface of the leaves, both of which are related to further environmental conditions. Stomatal uptake was found to depend on the photosynthetic activity, turgor pressure, and removal time in the intercellular spaces, particularly for O_3 and NO_2, which were almost immediately metabolized [4]. Therefore, stomatal uptake through stomata could possibly be influenced by drought stress, which the standard i-Tree Eco model neglects, assuming sufficient water availability or irrigation for the street and park trees. In fact, the stomatal closure has been shown to considerably reduce pollution removal in dry periods and alternative model formulations have been suggested [80,81]. Consequently, surface deposition was found to strongly depend on leaf structure [82,83], which determines both velocity and deposition capacity. Deposition capacity in turn is also dynamical, since washing the deposited content from the leaf reduces the pollutant storage at the leaves [84]. In the case of NO_2 and SO_2, it is also possible that pollution removal occurs by means of dissolving directly into the water film on the plant surface [4]. Although it might have a minor impact compared with the influence of the stomata on the gaseous uptake, the uncertainty associated with leaf-surface properties and the dependency on rainfall are currently underexplored in i-Tree Eco.

In addition, pollutant deposition varies with the canopy structure and tree position because these factors determine the air flow within and around trees [85]. However, the relation between tree traits (e.g., crown geometry and foliage distribution), "urban street canyon", and weather conditions are complex and cannot be evaluated using i-Tree Eco. For example, low turbulence may promote deposition and increase the N_2O and CO concentrations or O_3 formation due to longer residence time [86].

Based on the above discussion, it can be easily observed that i-Tree Eco estimates constitute a relatively first-order approximation that is solely related to surface area and uses lumped velocity parameters for pollutants that are nevertheless species specific. Only CO removal is independent of LA, possibly because it is independent of photosynthesis and transpiration [52,87]. This assumption is likely to be defensible because CO deposition in soil has been demonstrated to be considerably larger than that in plant leaves [48,88].

5. Conclusions

Englischer Garten trees provide important ecosystem services to Munich. The results of our model simulation revealed that in 2012, they potentially removed 4 t of pollutants, particularly ozone and nitrogen dioxide, and more than 200 t of carbon dioxide. The robustness of the model estimates was found to strongly depend on accurate species-specific parametrization as well as an individual determination of the competition state of the trees. The suggested automated determination process represents an objective procedure that is in many ways preferable to manual investigations, although its applicability and precision remains to be tested against field observations. Species-specific parameterization is particularly necessary for the determination of BVOC emissions. Since the taxonomic approach of i-Tree Eco only assigns genus or family values, simulations have uncertainties associated with species that differ from the genus- or dominating species-based settings, even if their abundance is relatively small. Therefore, it is strongly recommended to complement remote sensing applications with terrestrial observations and improve the database of species-specific parameters. Overall, we highlighted a considerable potential for improvements in the i-Tree Eco model process representations, particularly concerning the climate sensitivity of emission and growth processes.

Acknowledgments: This research was supported by Graduate School for Climate and Environment (GRACE). We also acknowledge support by Deutsche Forschungsgemeinschaft and Open Access Publishing Fund of Karlsruhe Institute of Technology. Furthermore, we thank the Bavarian Administration of State-Owned Palaces, Gardens and Lakes for providing the individual tree data, the Bavarian Environment Agency (LFU) for providing air pollution data, the i-Tree support team for assisting us in model implementation and data processing, and the Graduiertenzentrum Weihenstephan of Technical University of Munich and the ENAGO company for the English editing.

Author Contributions: R.P. performed the simulation experiments and analyzed the data; R.P. and R.G. conceived and designed the experiments and jointly wrote the text; P.B. and H.P. provided the competition algorithm, supported the implementation, and revised the text.

Conflicts of Interest: The authors declare no conflict of interest.

References

1. United Nations. *World Urbanization Prospects: The 2014 Revision, Highlights (ST/ESA/SER.A/352)*; Department of Economic and Social Affairs, Population Division: New York, NY, USA, 2014; ISBN 9789211515176.
2. UN-Habitat. *Urbanization and Development: Emerging Futures. World Cities Report 2016*; United Nations Human Settlements Programme: Nairobi, Kenya, 2016; ISBN 978-92-1-132708-3.
3. Salbitano, F.; Borelli, S.; Conigliaro, M.; Chen, Y. *Guidelines on Urban and Peri-Urban Forestry*; FAO Forest; Food and Agriculture Organization of the United Nations: Rome, Italy, 2016; ISBN 9789251094426.
4. Grote, R.; Samson, R.; Alonso, R.; Amorim, J.H.; Cariñanos, P.; Churkina, G.; Fares, S.; Thiec, D.L.; Niinemets, Ü.; Mikkelsen, T.N.; et al. Functional traits of urban trees: Air pollution mitigation potential. *Front. Ecol. Environ.* **2016**, *14*, 543–550. [CrossRef]
5. Churkina, G.; Grote, R.; Butler, T.M.; Lawrence, M. Natural selection? Picking the right trees for urban greening. *Environ. Sci. Policy* **2015**, *47*, 12–17. [CrossRef]
6. Maes, J.; Egoh, B.; Willemen, L.; Liquete, C.; Vihervaara, P.; Schägner, J.P.; Grizzetti, B.; Drakou, E.G.; Notte, A.L.; Zulian, G.; et al. Mapping ecosystem services for policy support and decision making in the European Union. *Ecosyst. Serv.* **2012**, *1*, 31–39. [CrossRef]
7. Endreny, T.; Santagata, R.; Perna, A.; De Stefano, C.; Rallo, R.F.; Ulgiati, S. Implementing and managing urban forests: A much needed conservation strategy to increase ecosystem services and urban wellbeing. *Ecol. Modell.* **2017**, *360*, 328–335. [CrossRef]
8. Nowak, D.; Crane, D. The urban forest effects (UFORE) model: Quantifying urban forest structure and function. In *Integrated Tools for Natural Resources Inventories in the 21st Century*; Hansen, M., Burk, T., Eds.; U.S. Department of Agriculture, Forest Service, North Central Forest Experiment Station: Saint Paul, MN, USA, 1998; pp. 714–720.

9. Hirabayashi, S.; Kroll, C.N.; Nowak, D.J. Development of a distributed air pollutant dry deposition modeling framework. *Environ. Pollut.* **2012**, *171*, 9–17. [CrossRef] [PubMed]
10. Nowak, D.J.; Hoehn, R.E.; Bodine, A.R.; Greenfield, E.J.; O'Neil-Dunne, J. Urban forest structure, ecosystem services and change in Syracuse, NY. *Urban Ecosyst.* **2013**, *19*, 1–23. [CrossRef]
11. Russo, A.; Escobedo, F.J.; Zerbe, S. Quantifying the local-scale ecosystem services provided by urban treed streetscapes in Bolzano, Italy. *AIMS Environ. Sci.* **2016**, *3*, 58–76. [CrossRef]
12. Selmi, W.; Weber, C.; Rivière, E.; Blond, N.; Mehdi, L.; Nowak, D. Air pollution removal by trees in public green spaces in Strasbourg city, France. *Urban For. Urban Green.* **2016**, *17*, 192–201. [CrossRef]
13. Westfall, J. Spatial-scale considerations for a large-area forest inventory regression model. *Forestry* **2015**, *88*, 267–274. [CrossRef]
14. Nowak, D.J.; Walton, J.; Stevens, J.C.; Crane, D.E.; Hoehn, R.E. Effect of Plot and Sample Size on Timing and Precision of Urban Forest Assessments METHODS Effect of Plot Size on Data Collection Time and Total Population Estimate Precision. *Arboric. Urban For.* **2008**, *34*, 386–390.
15. Bottalico, F.; Chirici, G.; Giannetti, F.; De Marco, A.; Nocentini, S.; Paoletti, E.; Salbitano, F.; Sanesi, G.; Serenelli, C.; Travaglini, D. Air Pollution Removal by Green Infrastructures and Urban Forests in the City of Florence. *Agric. Agric. Sci. Procedia* **2016**, *8*, 243–251. [CrossRef]
16. Manes, F.; Marando, F.; Capotorti, G.; Blasi, C.; Salvatori, E.; Fusaro, L.; Ciancarella, L.; Mircea, M.; Marchetti, M.; Chirici, G.; et al. Regulating Ecosystem Services of forests in ten Italian metropolitan Cities: Air quality improvement by PM_{10} and O_3 removal. *Ecol. Indic.* **2016**, *67*, 425–440. [CrossRef]
17. Marando, F.; Salvatori, E.; Fusaro, L.; Manes, F. Removal of PM_{10} by forests as a nature-based solution for air quality improvement in the Metropolitan city of Rome. *Forests* **2016**, *7*, 150. [CrossRef]
18. Fusaro, L.; Marando, F.; Sebastiani, A.; Capotorti, G.; Blasi, C.; Copiz, R.; Congedo, L.; Munafò, M.; Ciancarella, L.; Manes, F. Mapping and Assessment of PM_{10} and O_3 Removal by Woody Vegetation at Urban and Regional Level. *Remote Sens.* **2017**, *9*, 791. [CrossRef]
19. Bechtold, W.A. Crown position and light exposure classification-an alternative to field-assigned crown class. *North. J. Appl. For.* **2003**, *20*, 154–160.
20. Alonzo, M.; Bookhagen, B.; Roberts, D.A. Urban tree species mapping using hyperspectral and LiDAR data fusion. *Remote Sens. Environ.* **2014**, *148*, 70–83. [CrossRef]
21. Alonzo, M.; McFadden, J.P.; Nowak, D.J.; Roberts, D.A. Mapping urban forest structure and function using hyperspectral imagery and LiDAR data. *Urban For. Urban Green.* **2016**, *17*, 135–147. [CrossRef]
22. Parmehr, E.G.; Amati, M.; Taylor, E.J.; Livesley, S.J. Estimation of urban tree canopy cover using random point sampling and remote sensing methods. *Urban For. Urban Green.* **2016**, *20*, 160–171. [CrossRef]
23. Shojanoori, R.; Shafri, H.Z.M. Review on the Use of Remote Sensing for Urban Forest Monitoring. *Arboric. Urban For.* **2016**, *42*, 400–417.
24. Yang, J.; Chang, Y.M.; Yan, P.B. Ranking the suitability of common urban tree species for controlling $PM_{2.5}$ pollution. *Atmos. Pollut. Res.* **2015**, *6*, 267–277. [CrossRef]
25. Fassnacht, F.E.; Latifi, H.; Stereńczak, K.; Modzelewska, A.; Lefsky, M.; Waser, L.T.; Straub, C.; Ghosh, A. Review of studies on tree species classification from remotely sensed data. *Remote Sens. Environ.* **2016**, *186*, 64–87. [CrossRef]
26. Berland, A.; Lange, D.A. Google Street View shows promise for virtual street tree surveys. *Urban For. Urban Green.* **2017**, *21*, 11–15. [CrossRef]
27. Tanhuanpää, T.; Vastaranta, M.; Kankare, V.; Holopainen, M.; Hyyppä, J.; Hyyppä, H.; Alho, P.; Raisio, J. Mapping of urban roadside trees—A case study in the tree register update process in Helsinki City. *Urban For. Urban Green.* **2014**, *13*, 562–570. [CrossRef]
28. Bella, I.E. A new competition model for individual trees. *For. Sci.* **1971**, *17*, 364–372.
29. Korol, R.L.; Running, S.W.; Milner, K.S. Incorporating intertree competition into an ecosystem model. *Can. J. For. Res.* **1995**, *25*, 413–424. [CrossRef]
30. Fox, J.C.; Bi, H.; Ades, P.K. Spatial dependence and individual-tree growth models. II. Modelling spatial dependence. *For. Ecol. Manag.* **2007**, *245*, 20–30. [CrossRef]
31. Pretzsch, H.; Biber, P.; Dursky, J. The single tree-based stand simulator SILVA: Construction, application and evaluation. *For. Ecol. Manag.* **2002**, *162*, 3–21. [CrossRef]
32. Nowak, D.J.; Crane, D.E.; Stevens, J.C.; Hoehn, R.E.; Walton, J.T.; Bond, J. A Ground-Based Method of Assessing Urban Forest Structure and Ecosystem Services. *Arboric. Urban For.* **2008**, *34*, 347–358. [CrossRef]

33. USDA Forest Service. *i-Tree Eco User's Manual v 6.0*; U.S. Forest Service Northern Research Station (NRS): Washington, DC, USA, 2016.
34. Nowak, D.I. Estimating Leaf Area and Leaf Biomass of Open-Grown Deciduous Urban Trees. *For. Sci.* **1996**, *42*, 504–507.
35. Nowak, D.J.; Crane, D.E. Carbon storage and sequestration by urban trees in the USA. *Environ. Pollut.* **2002**, *116*, 381–389. [CrossRef]
36. BMEL Federal Ministry of Food and Agriculture. *The Forests in Germany: Selected Results of the Third National Forest Inventory*; Federal Ministry of Food and Agriculture: Berlin, Germany, 2015.
37. Hirabayashi, S. *Air Pollutant Removals, Biogenic Emissions and Hydrologic Estimates for i-Tree Applications*; United States Forest Service: Syracuse, NY, USA, 2016.
38. Nowak, D.J. Atmospheric Carbon Dioxide Reduction by Chicago's urban forest. In *Chicago's Urban Forest Ecosystem: Results of the Chicago Urban Forest Climate Project*; McPherson, E.G., Nowak, D.J., Eds.; US Department of Agriculture, Forest Service, Northeastern Forest Experiment Station: Radnor, PA, USA, 1994; pp. 83–94.
39. Cairns, M.A.; Brown, S.; Helmer, E.H.; Baumgardner, G.A. Root biomass allocation in the world's upland forests. *Oecologia* **1997**, *111*, 1–11. [CrossRef] [PubMed]
40. Hirabayashi, S.; Kroll, C.N.; Nowak, D.J. Component-based development and sensitivity analyses of an air pollutant dry deposition model. *Environ. Model. Softw.* **2011**, *26*, 804–816. [CrossRef]
41. Nowak, D.J.; Crane, D.E.; Stevens, J.C. Air pollution removal by urban trees and shrubs in the United States. *Urban For. Urban Green.* **2006**, *4*, 115–123. [CrossRef]
42. Nowak, D.J.; Hirabayashi, S.; Bodine, A.; Hoehn, R. Modeled $PM_{2.5}$ removal by trees in ten US cities and associated health effects. *Environ. Pollut.* **2013**, *178*, 395–402. [CrossRef] [PubMed]
43. Nowak, D.J.; Hirabayashi, S.; Bodine, A.; Greenfield, E. Tree and forest effects on air quality and human health in the United States. *Environ. Pollut.* **2014**, *193*, 119–129. [CrossRef] [PubMed]
44. Baldocchi, D.D.; Hicks, B.B.; Camara, P. A canopy stomatal resistance model for gaseous deposition to vegetated surfaces. *Atmos. Environ.* **1987**, *21*, 91–101. [CrossRef]
45. Pederson, J.R.; Massman, W.J.; Mahrt, L.; Delany, A.; Oncley, S.; Hartog, G.D.; Neumann, H.H.; Mickle, R.E.; Shaw, R.H.; Paw U, K.T.; et al. California ozone deposition experiment: Methods, results, and opportunities. *Atmos. Environ.* **1995**, *29*, 3115–3132. [CrossRef]
46. Hirabayashi, S.; Kroll, C.N.; Nowak, D.J. *i-Tree Eco Dry Deposition Model Descriptions*; United States Forest Service: Syracuse, NY, USA, 2015.
47. Baldocchi, D. A Multi-layer model for estimating sulfur dioxide deposition to a deciduous oak forest canopy. *Atmos. Environ.* **1988**, *22*, 869–884. [CrossRef]
48. Hosker, R.P.; Lindberg, S.E. Review: Atmospheric deposition and plant assimilation of gases and particles. *Atmos. Environ.* **1982**, *16*, 889–910. [CrossRef]
49. Wesley, M.L. Parametrization of surface resistance to gaseous dry deposition in regional-scale numerical model. *Atmos. Environ.* **1989**, *23*, 1293–1304. [CrossRef]
50. Taylor, G.E.; Hanson, P.J.; Baldocchi, D.D. Pollutant deposition to individual leaves and plant canopies: Sites of regulation and relationship to injury. In *Assessment of Crop Loss from Air Pollution*; Heck, W.W., Taylor, O.C., Tingey, D.T., Eds.; Springer: Dordrecht, The Netherlands, 1988; pp. 227–257.
51. Lovett, G.M. Atmospheric deposition of nutrients and pollutants in North America: An ecological perspective. *Ecol. Appl.* **1994**, *4*, 629–650. [CrossRef]
52. Bidwell, R.G.S.; Fraser, D.E. Carbon monoxide uptake and metabolism by leaves. *Can. J. Bot.* **1972**, *50*, 1435–1439. [CrossRef]
53. Guenther, A.B.; Zimmerman, P.R.; Harley, P.C.; Monson, R.K. Isoprene and Monoterpene Emission Rate Variability' Model Evaluations and Sensitivity Analyses. *J. Geophys. Res.* **1993**, *98617*, 609–612. [CrossRef]
54. Geron, C.D.; Guenther, A.B.; Pierce, T.E. An improved model for estimating emissions of volatile organic compounds from forests in the eastern United States. *J. Geophys. Res.* **1994**, *99*, 12773. [CrossRef]
55. Hirabayashi, S. *i-Tree Eco Biogenic Emissions Model Descriptions*; United States Forest Service: Syracuse, NY, USA, 2012.
56. Nowak, D.J.; Crane, D.E.; Stevens, J.C.; Ibarra, M. *Brooklyn's Urban Forest*; U.S. Department of Agriculture, Forest Service, Northeastern Research Station: Newtown Square, PA, USA, 2002.
57. Monteith, J.L.; Unsworth, M.H. *Principles of Environmental Physics*, 2nd ed.; Edward Arnold: London, UK, 1990.

58. Rogers, K.; Sacre, K.; Goodenough, J.; Doick, K. *Valuing London's Urban Forest*; Treeconomics: London, UK, 2015; ISBN 9780957137110.
59. Grantz, D.A.; Gunn, S.; Vu, H.B. O_3 impacts on plant development: A meta-analysis of root/shoot allocation and growth. *Plant Cell Environ.* **2006**, *29*, 1193–1209. [CrossRef] [PubMed]
60. Landolt, W.; Bühlmann, U.; Bleuler, P.; Bucher, J.B. Ozone exposure–response relationships for biomass and root/shoot ratio of beech (*Fagus sylvatica*), ash (*Fraxinus excelsior*), Norway spruce (*Picea abies*) and Scots pine (Pinus sylvestris). *Environ. Pollut.* **2000**, *109*, 473–478. [CrossRef]
61. Moser, A.; Rötzer, T.; Pauleit, S.; Pretzsch, H. The Urban Environment Can Modify Drought Stress of Small-Leaved Lime (*Tilia cordata* Mill.) and Black Locust (*Robinia pseudoacacia* L.). *Forests* **2016**, *7*, 71. [CrossRef]
62. Pretzsch, H.; Biber, P.; Uhl, E.; Dahlhausen, J.; Schütze, G.; Perkins, D.; Rötzer, T.; Caldentey, J.; Koike, T.; van Con, T.; et al. Climate change accelerates growth of urban trees in metropolises worldwide. *Sci. Rep.* **2017**, *7*, 15403. [CrossRef] [PubMed]
63. Dahlhausen, J.; Rötzer, T.; Biber, P.; Uhl, E.; Pretzsch, H. Urban climate modifies tree growth in Berlin. *Int. J. Biometeorol.* **2017**, 1–14. [CrossRef] [PubMed]
64. McHale, M.R.; Burke, I.C.; Lefsky, M.A.; Peper, P.J.; McPherson, E.G. Urban forest biomass estimates: Is it important to use allometric relationships developed specifically for urban trees? *Urban Ecosyst.* **2009**, *12*, 95–113. [CrossRef]
65. Russo, A.; Escobedo, F.J.; Timilsina, N.; Schmitt, A.O.; Varela, S.; Zerbe, S. Assessing urban tree carbon storage and sequestration in Bolzano, Italy. *Int. J. Biodivers. Sci. Ecosyst. Serv. Manag.* **2014**, *10*, 54–70. [CrossRef]
66. König, G.; Brunda, M.; Puxbaum, H.; Hewitt, C.N.; Duckham, S.C.; Rudolph, J. Relative contribution of oxygenated hydrocarbons to the total biogenic VOC emissions of selected mid-European agricultural and natural plant species. *Atmos. Environ.* **1995**, *29*, 861–874. [CrossRef]
67. Moukhtar, S.; Bessagnet, B.; Rouil, L.; Simon, V. Monoterpene emissions from Beech (*Fagus sylvatica*) in a French forest and impact on secondary pollutants formation at regional scale. *Atmos. Environ.* **2005**, *39*, 3535–3547. [CrossRef]
68. Aydin, Y.M.; Yaman, B.; Koca, H.; Dasdemir, O.; Kara, M.; Altiok, H.; Dumanoglu, Y.; Bayram, A.; Tolunay, D.; Odabasi, M.; et al. Biogenic volatile organic compound (BVOC) emissions from forested areas in Turkey: Determination of specific emission rates for thirty-one tree species. *Sci. Total Environ.* **2014**, *490*, 239–253. [CrossRef] [PubMed]
69. Papiez, M.R.; Potosnak, M.J.; Goliff, W.S.; Guenther, A.B. The impacts of reactive terpene emissions from plants on air quality in Las Vegas, Nevada. *Atmos. Environ.* **2009**, *43*, 4109–4123. [CrossRef]
70. Tiwary, A.; Namdeo, A.; Fuentes, J.; Dore, A.; Hu, X.; Bell, M. Systems scale assessment of the sustainability implications of emerging green initiatives. *Environ. Pollut.* **2013**, *183*, 213–223. [CrossRef] [PubMed]
71. Curtis, A.J.; Helmig, D.; Baroch, C.; Daly, R.; Davis, S. Biogenic volatile organic compound emissions from nine tree species used in an urban tree-planting program. *Atmos. Environ.* **2014**, *95*, 634–643. [CrossRef]
72. Dunn-Johnston, K.A.; Kreuzwieser, J.; Hirabayashi, S.; Plant, L.; Rennenberg, H.; Schmidt, S. Isoprene Emission Factors for Subtropical Street Trees for Regional Air Quality Modeling. *J. Environ. Qual.* **2016**, *45*, 234–243. [CrossRef] [PubMed]
73. Monson, R.K.; Grote, R.; Niinemets, Ü.; Schnitzler, J.P. Modeling the isoprene emission rate from leaves. *New Phytol.* **2012**, *195*, 541–559. [CrossRef] [PubMed]
74. Ghirardo, A.; Xie, J.; Zheng, X.; Wang, Y.; Grote, R.; Block, K.; Wildt, J.; Mentel, T.; Kiendler-Scharr, A.; Hallquist, M.; et al. Urban stress-induced biogenic VOC emissions and SOA-forming potentials in Beijing. *Atmos. Chem. Phys.* **2016**, *16*, 2901–2920. [CrossRef]
75. Grote, R.; Lavoir, A.V.; Rambal, S.; Staudt, M.; Zimmer, I.; Schnitzler, J.P. Modelling the drought impact on monoterpene fluxes from an evergreen Mediterranean forest canopy. *Oecologia* **2009**, *160*, 213–223. [CrossRef] [PubMed]
76. Bourtsoukidis, E.; Kawaletz, H.; Radacki, D.; Schütz, S.; Hakola, H.; Hellén, H.; Noe, S.; Mölder, I.; Ammer, C.; Bonn, B. Impact of flooding and drought conditions on the emission of volatile organic compounds of *Quercus robur* and *Prunus serotina*. *Trees* **2014**, *28*, 193–204. [CrossRef]
77. Derwent, R.G.; Jenkin, M.E.; Saunders, S.M. Photochemical ozone creation potentials for a large number of reactive hydrocarbons under European conditions. *Atmos. Environ.* **1996**, *30*, 181–199. [CrossRef]

78. Cabaraban, M.T.I.; Kroll, C.N.; Hirabayashi, S.; Nowak, D.J. Modeling of air pollutant removal by dry deposition to urban trees using a WRF/CMAQ/i-Tree Eco coupled system. *Environ. Pollut.* **2013**, *176*, 123–133. [CrossRef] [PubMed]
79. McPherson, E.; Peper, P. Urban tree growth modeling. *Arboric. Urban For.* **2012**, *38*, 172–180.
80. Fares, S.; Savi, F.; Muller, J.; Matteucci, G.; Paoletti, E. Simultaneous measurements of above and below canopy ozone fluxes help partitioning ozone deposition between its various sinks in a Mediterranean Oak Forest. *Agric. For. Meteorol.* **2014**, *198*, 181–191. [CrossRef]
81. Morani, A.; Nowak, D.; Hirabayashi, S.; Guidolotti, G.; Medori, M.; Muzzini, V.; Fares, S.; Mugnozza, G.S.; Calfapietra, C. Comparing i-Tree modeled ozone deposition with field measurements in a periurban Mediterranean forest. *Environ. Pollut.* **2014**, *195*, 202–209. [CrossRef] [PubMed]
82. Beckett, K.P.; Freer-Smith, P.H.; Taylor, G. Particulate pollution capture by urban trees: Effect of species and windspeed. *Glob. Chang. Biol.* **2000**, *6*, 995–1003. [CrossRef]
83. Kardel, F.; Wuyts, K.; Babanezhad, M.; Wuytack, T.; Adriaenssens, S.; Samson, R. Tree leaf wettability as passive bio-indicator of urban habitat quality. *Environ. Exp. Bot.* **2012**, *75*, 277–285. [CrossRef]
84. Hofman, J.; Wuyts, K.; Van Wittenberghe, S.; Samson, R. On the temporal variation of leaf magnetic parameters: Seasonal accumulation of leaf-deposited and leaf-encapsulated particles of a roadside tree crown. *Sci. Total Environ.* **2014**, *493*, 766–772. [CrossRef] [PubMed]
85. Amorim, J.H.; Rodrigues, V.; Tavares, R.; Valente, J.; Borrego, C. CFD modelling of the aerodynamic effect of trees on urban air pollution dispersion. *Sci. Total Environ.* **2013**, *461–462*, 541–551. [CrossRef] [PubMed]
86. Harris, T.B.; Manning, W.J. Nitrogen dioxide and ozone levels in urban tree canopies. *Environ. Pollut.* **2010**, *158*, 2384–2386. [CrossRef] [PubMed]
87. Pihlatie, M.; Rannik, Ü.; Haapanala, S.; Peltola, O.; Shurpali, N.; Martikainen, P.J.; Lind, S.; Hyvönen, N.; Virkajärvi, P.; Zahniser, M.; et al. Seasonal and diurnal variation in CO fluxes from an agricultural bioenergy crop. *Biogeosciences* **2016**, *13*, 5471–5485. [CrossRef]
88. Sanhueza, E.; Dong, Y.; Scharffe, D.; Lobert, J.M.; Crutzen, P.J.; Dong, Y.; Scharffe, D.; Lobert, J.M.; Carbon, P.J.C. Carbon monoxide uptake by temperate forest soils: The effects of leaves and humus layers. *Tellus B Chem. Phys. Meteorol.* **1998**, *50*, 51–58. [CrossRef]

© 2018 by the authors. Licensee MDPI, Basel, Switzerland. This article is an open access article distributed under the terms and conditions of the Creative Commons Attribution (CC BY) license (http://creativecommons.org/licenses/by/4.0/).